Romanian Reports in Physics **70**, 802 (2018)

INTEGRATED METHODOLOGY FOR THE NON-DESTRUCTIVE CHARACTERIZATION OF CULTURAL HERITAGE ARTIFACTS

I. FIERASCU[1], R.C. FIERASCU[1*], A. ORTAN[1,2], D.A. MIREA[3], C. MORARESCU[3]

[1] National R&D Institute for Chemistry and Petrochemistry – ICECHIM Bucharest, 202 Spl. Independentei, 060021 Bucharest, Romania
[2] University of Agronomic Sciences and Veterinary Medicine of Bucharest, 59 Marasti Blvd., 011464 Bucharest, Romania
[3] "Horia Hulubei" National Institute for Nuclear Physics and Engineering, 30 Reactorului Str., 077125 Magurele, Ilfov, Romania
[*]Corresponding author: *radu_claudiu_fierascu@yahoo.com*

Received December 4, 2017

Abstract. Data available in the literature often presents micro-area results from a few points selected on the artifact, or *bulk* results referring to the whole studied material. The present study aims at an integrated approach, started with an optical microscopy evaluation to the complex *bulk* and *micro-area* characterization of selected metallic artifacts.

Key words: cultural heritage artifacts, nuclear techniques, analytical characterization.

1. INTRODUCTION

The study of the coins from the scientific point of view (characterizing analysis) may provide information on the minting technology of the period and of the economic development, suggestions regarding the provenance of the metal used and manufacturing type. The researchers have demonstrated since the development of modern analytical techniques and this interdisciplinary field that the chemical composition on the surface of old coins sometimes differs from that in the *bulk* [1, 2]. The cultural heritage artifacts in general (and metallic artifacts in particular) often need cleaning. However, application of unsuitable restoration techniques often leads to "over-cleaning" and, consequently, to irreparable aesthetic and historical value losses. To avoid such problems, a thorough characterization of the artifacts is necessary [3]. Literature data often presents either *bulk* results, referring to the entire studied material, or micro-area results, referring to selected points on the artifact [4, 5]. In this study, we present an integrated approach, starting from the microscopical evaluation (using optical microscopy) to the complex *bulk* and *micro-area* characterization of selected artifacts [6]. Even our research group demonstrated that the combined use of such techniques can provide information about the composition on the surface and in *bulk* [6]. Also, the selected techniques are useful in order to analyze the composition of the corrosion products or enrichment

of the alloy with other metals in different artifacts, as coins, statues, jewelry, etc. Thus, Ager *et al.* used micro-PIXE (Particle-induced X-ray emission) and XRF (X-Ray Fluorescence) in order to gain insight into the silver enrichment process [7], Ion *et al.* used XRF and XRD (X-Ray Diffraction) in the characterization of corrosion products on a piece of roman mirror [8], Gorghinian *et al.* applied XRF technique on ancient Roman imperial coins, in order to establish their composition and place/date of struck [9], Cristea-Stan *et al.* used both XRF and micro-PIXE for the investigation of ancient metallurgy [10], Radvan *et al.* used portable XRF for the investigation of certain bronze beads [11], while Constantinescu *et al.* [12] used PIXE and scanning electron microscopy equipped with energy dispersive X-Ray spectroscopy in studies on Transylvanian native gold samples.

The analysis of the metallic artifacts (especially coins) is important, in order to improve the use of related analytical techniques which can offer very good corroborated results, to introduce and produce a substantial and continue database, to determine the exact equivalence among the different denominations.

X-ray Fluorescence represents a standard method in archaeological science, can be a qualitative and quantitative technique, non-destructive, non-invasive, rapid and can provide the composition of the surface and the *bulk* material [13, 14]. X-ray Diffraction also represents a technique well established in the area of archaeometric studies. Especially when speaking of metal artifacts, XRD can offer valuable information regarding sample composition, as well as corrosion products forming at the surface of the artifacts [15].

In the last decades, PIXE emerged as a valuable method in the study of cultural heritage artifacts [16–19]. The technique can also offer information regarding the metal sources, by evaluating the trace elements present in the samples, but such conclusion must consider a series of factors influencing the metal traceability to the ore, one of the most important being the recycling process, commonly applied from the Ist century AD [6, 20].

In the present paper, we apply the proposed approach for the study of six Romanian coins issued between 1880 and 1914. The coins were selected considering, besides their origin, several other factors: all the coins belong to the same collection, thus having the same preservation conditions; all the coins have a relatively known composition; finally, the coins have a similar silver content. A combined approach using the selected techniques, regarded as complementary, can provide information about chemical and phase composition.

2. MATERIALS AND METHODS

2.1. NUMISMATIC MATERIALS

The coins subjected to study are depicted in Fig. 1, while Table 1 presents their general characteristics. All the coins belong to authors' private collection. The

analyses were performed without any cleaning, in order to evaluate both the composition and the corrosion products.

Fig. 1 – Analyzed coins (from left to right, up to down): sample 1–5 lei, 1880; sample 2–5 lei 1883; sample 3–1 leu, 1894; sample 4–1 leu, 1906; sample 5–5 lei, 1906; sample 6–2 lei, 1914.

Table 1

Characteristics of the analyzed coins. The standard composition presented refers to the composition presented by numismatic catalogues; further information can be found at *romaniancoins.org*

Sample	Inscription (obverse/reverse)	Diameter (mm)	Weight (g)	Standard composition (%)
Sample 1	*Carol I Domnul Romaniei / 5 L(ei), ROMANIA, 1880, Romanian coat of arms, letter B, Wheat spice*	37	24.98	Ag 90%, Cu 10%
Sample 2	*Carol I Rege al Romaniei / 5 L(lei), 1883, Romanian coat of arms, letter B, Wheat spice*	37	24.39	Ag 90%, Cu 10%
Sample 3	*Carol I Rege al Romaniei / 1 L(eu), 1894, Romanian coat of arms*	23	4.78	Ag 83.5%, Cu 16.5%
Sample 4	*Carol I Rege al Romaniei 1866-1906/ Carol I Domnul Romaniei 1 L(eu)*	23	4.86	Ag 83.5%, Cu 16.5%
Sample 5	*Carol I Rege al Romaniei 1866-1906/ Carol I Domnul Romaniei 5 L(ei)*	38	24.74	Ag 90%, Cu 10%
Sample 6	*Carol I Rege al Romaniei / Romania, 2 L(ei), 1914*	27	9.98	Ag 83.5%, Cu 16.5%

2.2. ANALYSIS METHODS

The preliminary evaluation of the coins was performed using a Kruss MBL3000 microscope, at different magnifications.

The nuclear analytical methods selected can be divided in two categories: ***bulk analyses*****:** *i)* Energy dispersive X-Ray Fluorescence, performed using EDXRF

Spectrometer PW4025 MiniPal 2, PANalytical, with a Si-PIN detector, at 20 kV and automatic current intensity, measurement time 300 s, in Helium atmosphere (beam spot area 81.7 mm^2); *ii)* X-Ray Diffraction performed using a Rigaku SmartLab 9 kW instrument, operating at 45 kV and 200 mA, using Cu Ka radiation (1.54059 Å), in parallel beam configuration (2θ/θ scan mode), from 10 to 90 2θ degrees; ***micro-area analyses:*** *i)* small spot Energy dispersive X-ray Fluorescence analyses were performed using a Bruker Tracer S1 Titan spectrometer. The spectrometer, equipped with a Rhodium anode tube, was used to generate a beam with the energy of 40 keV, that passed through a 3 mm collimator before reaching the samples. A Silicon Drift Detector (SDD) positioned at an angle of 45° with respect to the Rh-anode tube, was used to record the spectra. Four points randomly selected were analyzed on each coin, each point was exposed to the beam for a period of 40 s.; *ii)* micro-area X-Ray Diffraction analyses were performed using a Rigaku SmartLab 9 kW instrument, in *point focus* configuration, with *CBO-f* optics, estimated beam size – 400 μm, between 20 and 90 2θ degrees, on five points randomly selected; *iii)* Particle Induced X-Ray Emission analyses were performed at the "Horia Hulubei" National Institute for Physics and Nuclear Engineering using the 3MV Tandetron™ particle accelerator [21]. For the present study the newly developed "*In-Air*" PIXE setup was used. A 3 MeV proton beam obtained from the sputtering ion source and transported to the IBA (Ion Beam Analysis) chamber, was used to probe the samples. The proton beam spot size on the sample was about 1 mm in diameter.

The XRF results were analyzed using dedicated software of each instrument. The XRD results were analyzed using the Rigaku Data Analysis Software PDXL 2, database provided by ICDD, while the PIXE results were analyzed using the GUPIX software.

3. RESULTS AND DISCUSSION

The analyzed samples' preliminary observation was directed towards consistency evaluation of the general characteristics of the samples (shape of the letters, number of points on the pearl circle, emblem of the engraver, etc.) compared with the available literature data and the aspect of the corrosion points (Fig. 2).

The general characteristics of the coins evaluated do not arise any concerns regarding their authenticity. As expected from our previous studies regarding corrosion products of metallic artifacts [6, 8], three colors could be distinguished on the analyzed samples, corresponding to different corrosion products: black, reddish-brown and green (in few points).

The most probable corrosion products responsible for those colors are chlorargyrite and tenorite (black), cuprite (reddish brown), paratacamite or malachite (green) [6, 22, 23].

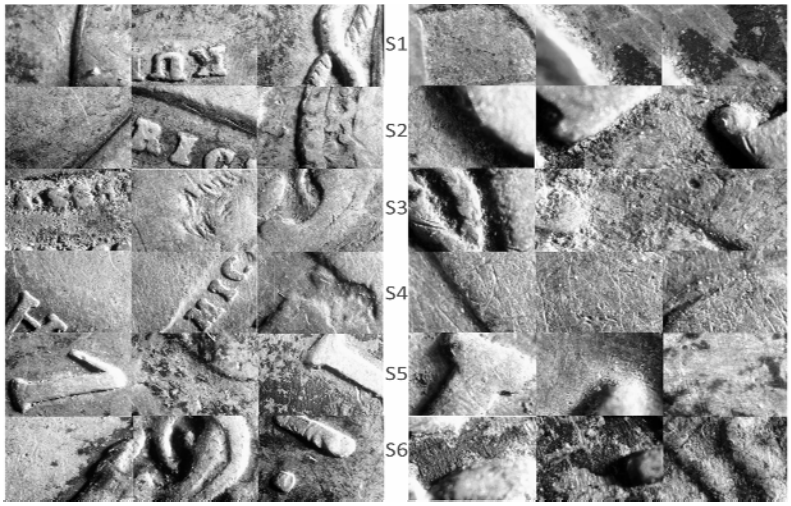

Fig. 2 – Surface features of the samples, observed by optical microscopy (40× – left; 100× – right) of samples 1 to 6.

As a second step of the study, the general composition of the samples was evaluated using the *bulk* analyses methods previously presented. The results are presented in Fig. 3 and Table 2.

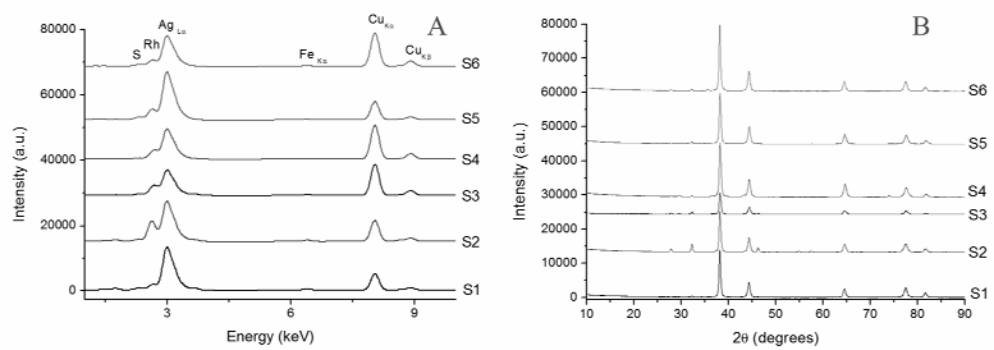

Fig. 3 – Results of the *bulk* analyses EDXRF spectra (A) and X-ray diffractograms (B).

The XRD analyses identified the diffraction peaks corresponding to the major component (the silver-copper alloy, ICDD PDF 04-010-7444) at 38.35, 44.47, 64.67, 77.47 and, respectively, 81.97 (2θ degrees) corresponding to (111), (200), (220), (311) and, respectively, (222) diffraction plane. The identification of the rest of the diffraction peaks confirmed the visual observation previously made. Thus, the peak at 28.02 (more visible for samples 2, 3 and 6) can be assigned to acanthite (ICDD PDF 04-008-7793) (200) plane, the peak at 29.6 degrees (more pronounced in sample 4) can be assigned to cuprite (ICDD PDF 01-075-4299) (110)/paratacamite

(ICDD PDF 04-011-3123) (401); the peak at 32.39 degrees can be assigned to chlorargyrite (ICDD PDF 04-012-6380) (200)/tenorite (ICDD 01-089-2531) (110)/ paratacamite (22-3); the peak from 36.2 degrees (samples 2, 4, 6) can be assigned to tenorite (002)/paratacamite (205); the peak appearing at 42.5 degrees can be assigned to cuprite (200)/paratacamite (23-4); the peak appearing at 46.2 degrees (more prominent in sample 2, but also appearing in the other samples) can be assigned to chlorargyrite (220)/tenorite (-112) /paratacamite (054); the peaks appearing at 54.8 degrees and, respectively, 57.5 degrees can be assigned to chlorargyrite (311)/paratacamite(407) and, respectively, chlorargyrite (222)/tenorite (202)/paratacamite (44-3); the peak appearing at 61.3 degrees and 73.6 degrees can be assigned to cuprite (220)/tenorite (-113)/paratacamite (048), respectively cuprite (311)/acanthite (422)/paratacamite (4010); finally, the peak appearing at 85.8 degrees can be assigned to cuprite (321)/chlorargyrite (422)/acanthite (440)/tenorite (130)/paratacamite (660).

Table 2

Bulk XRF results obtained for the analyzed coins

Sample	Element (%)								
	Si	S	Cl	Ca	Mn	Fe	Cu	Zn	Ag
1	1.2 ± 0.12	0.13 ± 0.002	1.1 ± 0.13	1.32 ± 0.13	0.03 ± 0.01	0.39 ± 0.02	6.2 ± 0.4	0.04 ± 0.01	89.1 ± 0.2
2	1.3 ± 0.18	0.98 ± 0.01	1.2 ± 0.21	0.96 ± 0.15	0.03 ± 0.01	0.27 ± 0.01	6.44 ± 0.3	0.08 ± 0.01	88.6 ± 0.3
3	1.4 ± 0.17	0.57 ± 0.005	1.3 ± 0.22	1.9 ± 0.22	0.01 ± 0.002	0.47 ± 0.02	11.2 ± 0.5	0.2 ± 0.05	80.65 ± 0.4
4	0.2 ± 0.02	0.43 ± 0.004	1.6 ± 0.28	0.47 ± 0.14	0.07 ± 0.01	0.18 ± 0.01	11.3 ± 0.6	0.08 ± 0.01	83.8 ± 0.3
5	0.58 ± 0.1	0.41 ± 0.003	1.8 ± 0.31	0.12 ± 0.01	0.01 ± 0.002	0.10 ± 0.01	6.21 ± 0.4	0.05 ± 0.01	89.6 ± 0.2
6	0.56 ± 0.1	0.32 ± 0.002	1.5 ± 0.21	0.21 ± 0.02	0.08 ± 0.01	0.23 ± 0.02	11.8 ± 0.6	0.08 ± 0.01	83.3 ± 0.2

The presence of minor elements detected in the samples can be explained by multiple mechanisms: they may originate from the ores used for manufacturing (or from the materials recycled to obtain the coins), they could be a result of contamination during manufacturing processes, or can originate from the preservation conditions (especially from burial) [6]. Considering the age of the analyzed samples, the last mechanism has little probability.

The XRD *small area* analysis aimed at highlighting the corrosion products found on the surface of the samples. From the diffractograms presented in Fig. 3, one can observe the increase in relative intensity of the peaks corresponding to corrosion products. This is explained by the experimental set-up chosen, that offers information mainly from the surface of the samples. Particularly, for each sample, the analysis of the results offers the following information: for Sample 1, the general aspect of the diffractograms is maintained for all the five points analysed. For all the points, a small peak around 26 degrees, corresponding to paratacamite (220) can be observed. Also, several other peaks can be attributed to corrosion products: 31.1 degrees – paratacamite (401); 33 degrees – paratacamite (22-3); 40 degrees –

paratacamite (404); 53 degrees (in points 1, 3 and 5) – paratacamite (440). Diffractograms obtained for sample 2 show more pronounced peaks of the corrosion products: 26 degrees (paratacamite (220)), especially for points 1, 2 and 3; point 6 also shows a peak at 43.05 degrees (2θ), that can be assigned to acanthite (-123); the peak around 46 degrees suffers a decrease in point 6, as well as the peaks around 55 and 57 degrees; another peak (around 68 degrees) can be seen in points 1 to 5, corresponding to tenorite (022).

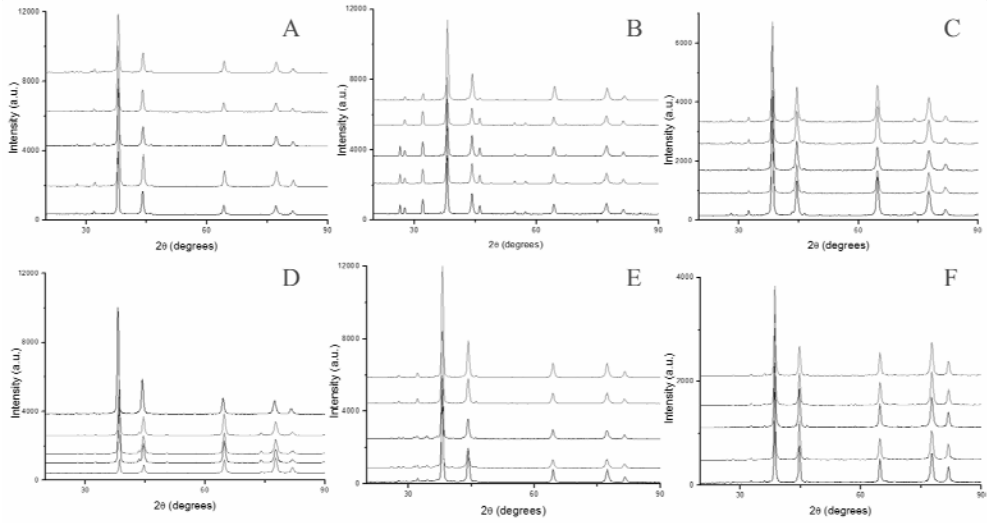

Fig. 4 – *Small area* XRD analysis of the samples (A to F – samples 1 to 6).

Sample 3 mainly presents the peaks already presented for *bulk* analyses. The peak around 30 degrees (already assigned to cuprite) is visible in points 1, 4 and 5. The peak at 46.2 degrees is now clearly visible for all analysed points; the peak at 85.8 degrees is only visible in point 5. Sample 4 presents variation of the peaks already presented (28.02, 32.39, 73.6 degrees); for points 1 to 4 is visible a peak at 50.03 degrees (2h), corresponding to paratacamite (603). Sample 5, besides the variation of some peaks already discussed, point 4 presents a small diffraction peaks around 26 degrees, corresponding to paratacamite (220); also, the peak at 46.2 degrees is visible in all points. Finally, sample 6 shows a new peak at 35 degrees (for points 1 and 3), corresponding to tenorite (-111).

A general observation that can be made regarding the results of the XRD *mapping* is related to the variation of the intensity of the peaks associated with the alloy planes. This variation in the diffraction profiles can offer information related to several characteristics, such as grain size or residual stress.

The micro-area analyses (PIXE and XRF) were performed to better understand the corrosion products, but also in order to evaluate the homogeneity of the samples. The results are presented in Table 3.

Table 3

Micro-area results (PIXE and XRF) obtained for the analyzed coins; N.D. – not detected.

Sample	Element (%)								
	Cl	Ca	Fe	Cu	Zn	Ag	Au	Pb	Ni
S. 1 XRF	N.D.	N.D.	N.D.	3.57 ± 0.135	0.36 ± 0.02	95.17 ± 1.02	N.D.	0.3 ± 0.125	0.08 ± 0.02
S.1 PIXE	0.2 ± 0.01	0.1 ± 0.008	0.01 ± 0.001	0.5 ± 0.008	N.D.	90.1 ± 1.21	0.3 ± 0.07	0.8 ± 0.05	N.D.
S.2 XRF	N.D.	N.D.	N.D.	4.06 ± 0.145	0.16 ± 0.02	95.33 ± 1.01	N.D.	0.13 ± 0.10	0.09 ± 0.02
S.2 PIXE	0.3 ± 0.01	0.1 ± 0.007	0.02 ± 0.003	1.1 ± 0.04	N.D.	91.3 ± 1.08	N.D.	0.01 ± 0.003	N.D.
S.3 XRF	N.D.	N.D.	N.D.	8.91 ± 0.21	0.13 ± 0.02	90.29 ± 0.96	N.D.	0.2 ± 0.11	0.08 ± 0.02
S.3 PIXE	0.2 ± 0.01	0.3 ± 0.01	0.03 ± 0.003	1.6 ± 0.01	N.D.	89.1 ± 1.14	0.3 ± 0.08	0.4 ± 0.05	N.D.
S.4 XRF	N.D.	N.D.	N.D.	9.2 ± 0.22	0.05 ± 0.02	90.13 ± 0.99	N.D.	0.33 ± 0.12	0.08 ± 0.02
S.4 PIXE	N.D.	1.1 ± 0.13	0.1 ± 0.02	17.7 ± 0.16	N.D.	91.1 ± 1.26	N.D.	0.03 ± 0.01	N.D.
S.5 XRF	N.D.	N.D.	N.D.	3.27 ± 0.13	0.11 ± 0.02	96.07 ± 1.01	N.D.	0.21 ± 0.11	0.072 ± 0.02
S.5 PIXE	0.2 ± 0.01	0.1 ± 0.008	0.01 ± 0.001	0.5 ± 0.008	N.D.	92.1 ± 1.24	0.3 ± 0.07	0.8 ± 0.005	N.D.
S.6 XRF	N.D.	N.D.	N.D.	8.62 ± 0.21	0.2 ± 0.025	90.64 ± 0.98	N.D.	0.1 ± 0.08	0.077 ± 0.02
S.6 PIXE	N.D.	0.1 ± 0.01	0.01 ± 0.002	1.8 ± 0.01	N.D.	91.1 ± 1.26	N.D.	N.D.	N.D.

Besides the elements presented in Table 3, by XRF were also determined some other trace elements, in some of the points analyzed: in Sample 1 were determined Cr (0.02%, in 1 point) and Hg (0.01%, in 1 point); in Sample 2 was determined Cr (0.02%, in 1 point); in Sample 3 were determined Cr (0.01%, in 1 point), Fe (0.21%, in 1 point), V (0.03%, in 1 point); in Sample 4 was determined Mn (0.01%, in 1 point); in Sample 6 was determined V (0.03%, in 1 point), Mn (0.015%, in 2 points) and Hg (0.015%, in 2 points).

As already mentioned in our previous study [6], the trace elements could be considered as indicators of the original silver source: zinc, lead gold, platinum, nickel and iron were found in Catalonian silver coins [24], while tin, lead, gold, platinum, bismuth, iron, chromium, nickel, zinc, manganese and titanium were found in Greek silver drachmae [25].

A main conclusion that could be drawn from the XRF and PIXE results is the fact the coins are relatively homogenous in composition (as can be seen from the small values of the standard deviation of the major elements). Another observation that can be made is that, due to their characteristics (both *small area* XRF and PIXE techniques are analyzing a very thin layer on the surface of the coins), the application of these methods alone, without any *bulk* analysis, will lead to significantly higher results for silver and lower for copper. This can be explained by the phenomenon of apparent silver surface enrichment [26].

4. CONCLUSIONS

The present paper proposes the combined use of different techniques (optical microscopy, *bulk* and *small area* XRD, *bulk* and *small area* XRF, PIXE) for the

evaluation of numismatic artifacts, in order to minimize the experimental errors that could arise from using the separate techniques. Six Romanian silver/copper coins were analyzed using the proposed approach, establishing their microscopic characteristics, chemical composition and corrosion products. It must be mentioned that the presented results are correlated with the experimental set-up used, as different set-ups of the same technique could result in a variation of the results.

Acknowledgments. This work was partially supported by a grant of the Romanian National Authority for Scientific Research and Innovation, CNCS/CCCDI-UEFISCDI, project number PN-III-P2-2.1-PED-2016-0198, within PNCDI III.

REFERENCES

1. J. Condamin and M. Picon, Archaeometry **7**, 98–105 (1964).
2. J. Condamin and M. Picon, *Methods of chemical and metallurgical investigation of ancient coinage*, Vol. 8, Royal Numismatic Society Special Publication, London, 1970.
3. T. Palomar, B.R. Barat, E. Garcia and E. Cano, J. Cult. Herit. **17**, 20–26 (2016).
4. J. Cruz, V. Corregidor and L.C. Alves, Nucl. Instrum. Methods Phys. Res. B, doi: 10.1016/ j.nimb.2017.02.010, (2017).
5. A.I. Moreno-Suarez, F.J. Ager, S. Scrivano, I. Ortega-Feliu, B. Gomez-Tubio and M.A. Respaldiz, Nucl. Instrum. Methods Phys. Res. B **358**, 93–97 (2015).
6. R.C. Fierascu, I. Fierascu, A. Ortan, C. Constantin, D.A. Mirea and M. Statescu, Nucl. Instrum. Methods Phys. Res. B **401**, 18–24 (2017).
7. F.J. Ager, A.I. Moreno-Suarez, S. Scrivano, I. Ortega-Feliu, B. Gomez-Tubio and M.A. Respaldiza, Nucl. Instrum. Methods Phys. Res. B **306,** 241–244 (2013).
8. R.M. Ion, I. Dumitriu, D. Boros, D. Isac, M.L. Ion, R.C. Fierascu and A. Catangiu, Metal. Int. **13**, 43–46 (2008).
9. A. Gorghinian, A. Esposito, M. Ferretti and F. Catalli, Nucl. Instrum. Methods Phys. Res. B **309**, 268–271 (2013).
10. D. Cristea-Stan, B. Constantinescu, G. Talmatchi and D. Ceccato, Rom. Journ. Phys. **61**(3–4), 445–456 (2016).
11. R. Radvan, C. Bors and L. Ghervase, Rom. Journ. Phys. **61**(9–10), 1530–1538 (2016).
12. B. Constantinescu, D. Cristea-Stan, D. Ceccato and C. Luculescu, Proc. Romanian Acad. A **18**(4), 308–314 (2017).
13. D. Cristea-Stan, B. Constantinescu, C. Chiojdeanu and C. A. Simion, Rom. Journ. Phys. **62**, 902 (2017).
14. S. Serafima, O.G. Duliu, M.M. Manea and G. Niculescu, Rom. Rep. Phys. **68**(1), 191–202 (2016).
15. H. Mousser, R. Amri, A. Madani, A. Darchen and A. Mousser, Appl. Surf. Sci. **257**, 5961–5965 (2011).
16. A. Vasilescu, B. Constantinescu, C. Chiojdeanu, D. Stan, R. Simon, D. Ceccato, A. Simon, Z. Kertesz, Z. Szikszai, I. Uzonyi, L. Csedreki and E. Furu, Rom. Rep. Phys. **65**, 1222–1233 (2013).
17. B. Constantinescu, V.J. Kennedy and G. Demortier, Int. J. PIXE **3–4**, 487–493 (1999).
18. M. Hajivalieia and F. Khademi Nadooshan, Nucl. Instrum. Methods Phys. Res. B **289**, 56–58 (2012).
19. R. Bugoi, I. Poll and Gh. Mănucu-Adameşteanu, Rom. Rep. Phys. **68**(3), 1004–1014 (2016).
20. L. Torrisi, A. Italiano and A. Torrisi, Appl. Surf. Sci. **387**, 529–538 (2016).

21. I. Burducea, M. Straticiuc, D.G. Ghita, D.V. Mosu, C.I. Calinescu, N.C. Podaru, D. Mous, I. Ursu and N.V. Zamfir, Nucl. Instrum. Methods Phys. Res. B **359**, 12–19 (2015).
22. J.C. D'Ars de Figueiredo, S.S. Asevedo and J.H.R. Barbosa, Appl. Surf. Sci. **317**, 67–72 (2014).
23. O. Abdel-Kareem, A. Al-Zahrani and M. Arbach, J. Archaeol. Sci. Rep. **9**, 565–576 (2016).
24. A. Pitarch, I. Queralt and A. Alvarez-Perez, Nucl. Instrum. Meth. Phys. Res. B **269**, 308–312 (2011).
25. Pitarch and I. Queralt, Nucl. Instrum. Meth. Phys. Res. B **268**, 1682–1685 (2010).
26. F.J. Ager, B. Gomez-Tubio, A. Paul, A. Gomez-Moron, S. Scrivano, I. Ortega-Feliu and M.A. Respaldiza, Microchem. J. **126**, 149–154 (2016).